

DESIGN OF AN INTEGRATED OPTICAL UNIT FOR LASER DOPPLER ANEMOMETRY

Eric Esteves Aderne*

Alcidney Valério Chaves†

José Luiz S. Neto†

Juliana B. R. Loureiro‡, jbrloureiro@gmail.com

*Physics Institute (IF/UFRJ),

† Electrical Engineering Program (COPPE/UFRJ),

‡ Mechanical Engineering Program (COPPE/UFRJ),

C.P. 68503, 21945-970, Rio de Janeiro, RJ, Brazil,

Abstract. *The objective of this work is to describe the design of an integrated optical unit for Laser Doppler Anemometry measurements. This unit allows the system to be operated either on forward or backscatter light collecting modes, depending on the geometrical arrangement of the optical components on the bench. The measurements shown here were obtained under controlled conditions to specifically investigate the performance of the proposed optical arrangement and components. The data acquisition system and mean velocity calculation is also discussed. Measurements show that the assembly of individual optical parts and the burst signal analysis performed in the present work led to an operational LDA system.*

Keywords: *Turbulence, Laser-Doppler Anemometry, Instrumentation, Experimental measurements*

1. INTRODUCTION

The first measurement technique that resorted to the Doppler effect to quantify the velocity of a fluid was developed by Yeh and Cummings (1964). Progressive advancements on electronics and optics contributed to establish the Laser Doppler Anemometry (LDA) as one of the most reliable and consolidated techniques for fluid flow and turbulence measurements.

Along the past decades, a number of papers can be found in the literature devoted to the working principles and operational details of the Laser Doppler Anemometry (LDA) technique, e. g., Durst and Whitelaw (1971), Knuhtsen et al. (1982), Tropea (1995) and Byrne et al. (2004). However, given the widespread use of commercial LDA systems for academic and scientific research purposes, it seems that most of the knowledge involved on the operation of different optical configurations for LDA is being lost. Durst and Whitelaw (1976), for example, highlight that reference beam mode is more suitable than the commonly used dual beam mode in flows where a high concentration of scattering particles are present.

Due to its particular characteristics of non-intrusiveness, intrinsically-calibrated linear response, high spatial and temporal resolution, the laser Doppler anemometry could be widely used for technological and industrial measurement purposes. However, the applicability of LDA systems has been restricted to the laboratory environment mainly because of the lack of portability of the commercial systems. Only a scarce number of special-purpose LDA systems has been developed for natural gas, naval and oceanographic deployment (e. g. Agrawal and Belting, 1988; Liu et al. 1992).

In this context, the knowledge involved in assembling and operating a LDA system from its very basic individual components is essential not only for scientific purposes but also for technological and industrial applications.

In addition, a remarkable and distinct characteristic of the laser-Doppler anemometry is its unique ability to resolve the viscous sublayer of classical and non-equilibrium turbulent boundary layers. It is of interest to note that for non-equilibrium flows the only reliable way to determine the local wall shear stress is to measure the velocity profile in the viscous sublayer. This method is even not violated by strong adverse pressure gradients and separated flows. Six wall shear stress measurement techniques are reviewed by Loureiro et al. (2010) for flow over a changing surface. Loureiro et

al. (2010) show that, through laser Doppler anemometry (LDA), ten points can be used to characterize the flow to within 500 μm of the wall.

This means that smaller measurement volumes imply greater spatial resolution and more accurate wall shear stress measurements. On the contrary of the restrictions imposed by the commercial systems, the ability to set up an integrated optical unit allows the user to adjust the measurement volume to the required size.

The purpose of this work is to design an integrated optical unit that can be operated either on the reference mode or in the dual beam configuration, depending on the geometrical arrangement of the optical components on the bench. The unit does also allow the measurements to be performed on forward and backscatter modes. The results shown here were obtained under controlled conditions to specifically investigate the performance of the proposed optical arrangement and components. Data acquisition and analysis software has been developed for converting the burst signals into mean velocity and further turbulence statistics. The advantage of this work is to gather complete knowledge on a state-of-the-art technique for fluid flow measurements, resulting in a self-contained and robust instrument capable of performing dedicated fluid flow experiments.

2. PRINCIPLES OF OPERATION

The classical dual-beam configuration is comprised of a laser source and series of transmitting optics that create two equally intense beams and make them cross in a point of space. Because of the coherence of the laser, the light intensity at this specific point varies from zero to a maximum in a sequential pattern, called the interference fringes. It should be noted that the fringes are equally spaced and its distance d_f depends only on the wavelength of the light source (λ) and on the angle between the two beams (θ) and can be written as

$$d_f = \frac{\lambda}{2 \sin \theta/2}. \tag{1}$$

eq:df

Small particles dispersed on the fluid move across the measurement volume and scatter light to the photodetector, which will convert the received photons into an electrical signal similar to the one illustrated in Fig. 1. The velocity of the fluid, which is assumed to be the local velocity of the seeding particles, can be calculated by the distance between the fringes and the time ($1/f_D$) the particle take to cross one pair of sequential fringes, where f_D is the Doppler frequency of the signal.

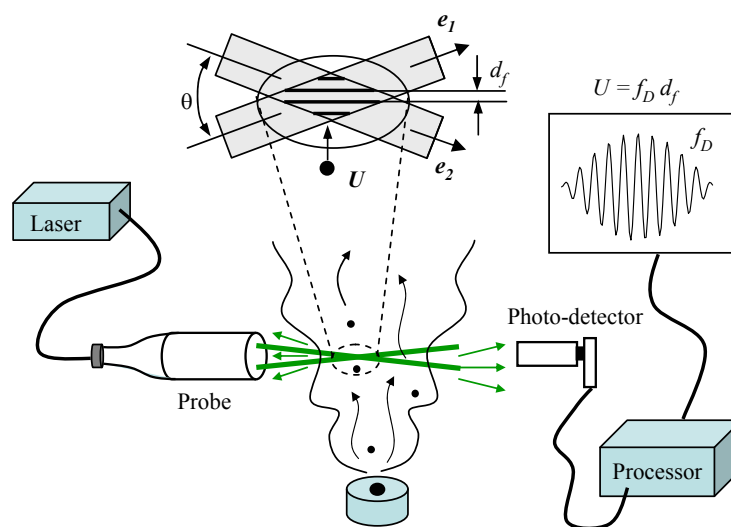


Figure 1. Illustration of the working principles of a Laser Doppler Anemometer.

fig:prin

This simplified interpretation of the system is based on the fringe model, proposed by Rudd (1969). This theoretical framework provides an easily visualized picture of the working principle and is the basis for both qualitative and quantitative analysis of the features of laser-Doppler signals. It can be shown that the frequency of the signals generated by the photodetector is exactly that determined from the analysis based on the Doppler effect considerations. As a consequence, we may write:

$$f_D = \frac{\vec{U}}{\lambda} \cdot (\vec{e}_1 - \vec{e}_2) = U_{\perp} \frac{2 \sin \theta/2}{\lambda}, \quad (2) \quad \text{eq:fD}$$

so that

$$U_{\perp} = f_D \lambda. \quad (3) \quad \text{eq:U}$$

It can be seen that the velocity component measured through the Doppler frequency is perpendicular to the fringe pattern, as shown in Fig. 1. The three components of the velocity field can then be easily measured by three individual probes correctly located on the flow field.

The fringe model also assures that the Doppler frequency measured from the scattered light is independent of the position of the photodetector, for the dual beam configuration mode. However, the signal quality and intensity do vary according to the location of the detector in relation to the emitting probe. This phenomena is related to the properties of the light scattered by small particles and define two main configurations for the collecting optics: i) the forward-scatter mode, where the photodetector is located on the opposite side of the emitted beams and ii) the backscatter mode, when the receiving optics is located inside the main probe.

The reference beam mode has been mostly used until late seventies, and its principal advantage has been its ease of alignment. In this configuration, one of the crossing beams is directed onto the photodetector. Further information on the working principles and optical configurations of an LDA system can be found in Durst, Melling and Whitelaw (1976) and Albrecht et al. (2003).

3. OPTICAL DESIGN

The optical arrangement of the designed LDA system operating in the dual beam mode configuration is presented in Fig. 2. A linearly polarized He-Ne laser of 10mW output power was chosen as the light source. This laser has a well stabilized wavelength (633 nm) assuring a good coherence length and high visibility for the interference fringes. The main beam provided by the laser is collimated and directed to a beam splitter specified to generate two beams of equal intensity for the current wavelength. After the beams pass through the transmitting lens of 100 mm focal length ($f = 100$ mm), the diameter of each beam continuously decreases to a minimum value at the focal point of the lens, called beam waist. In order to have a high quality interference fringes, the two beams should cross exactly at the beam waist. Should the two beams differ in light intensity, the wavefronts will not cancel each other (dark fringe) and the visibility of the fringes will be lowered. Figure 3 illustrates an image of the fringes obtained in this work, showing a sharp contrast between dark and bright areas, as well as the parallelism and equal spatial distribution of the projected fringes. High quality fringes tend to generate high signal to noise bursts as the one illustrated on the scope screen of Fig. 3(right).

As depicted in Fig. 2, the system was set to operate in the forward scatter mode to collect a higher intensity signal. A pair of receiving lenses was used to collimate and focus the scattered light onto the detector surface. The aperture in front of the receiver has the purpose to block stray light and spurious reflections and restrict the collection of light to a point corresponding to the measurement volume.

For the present configuration, the geometrical features of the system are given in Table 1.

For the purpose of conversion of scattered light into electrical signal, an avalanche photodiode (APD) was chosen.

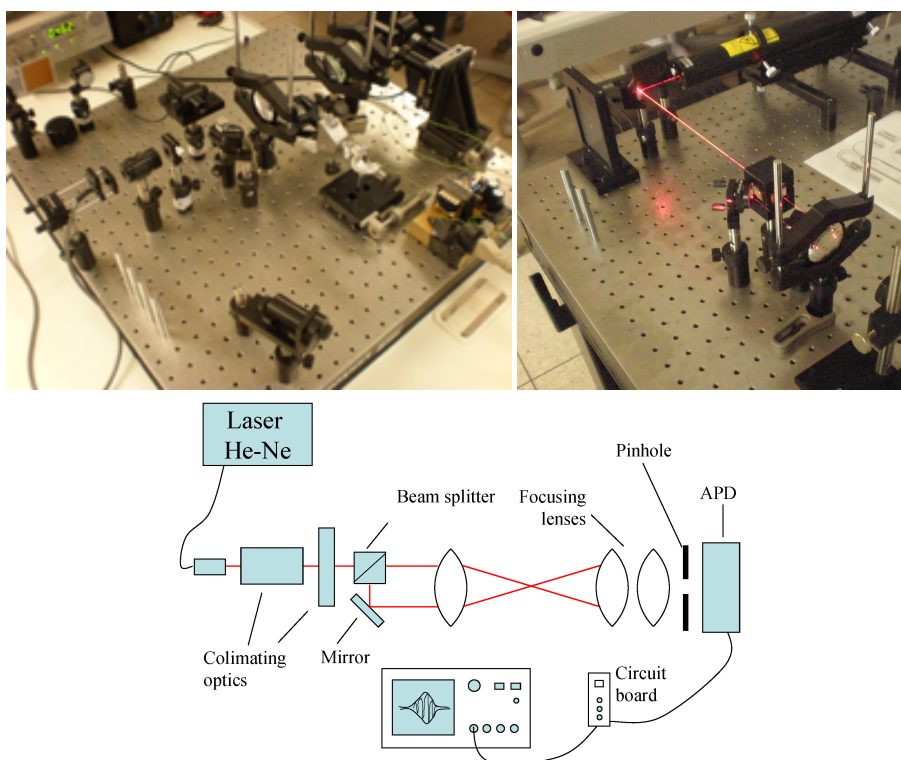


Figure 2. Overview of the optical components and geometrical arrangement of the system developed: (a) illustration of the optical table, (b) laser path before the beam splitter, (c) schematic diagram of the arrangement illustrated in (a).

fig:kitn

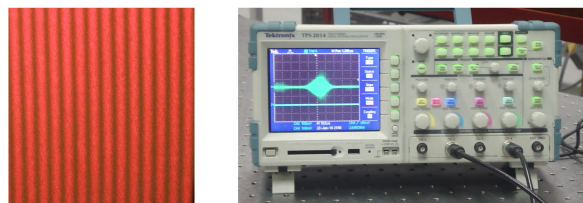


Figure 3. Illustration of the interference fringes and a typical burst signal on the scope.

fig:frin

Table 1. Main characteristics of the laser-Doppler system.

Wavelength	633 nm
Half-angle between beams	2.42°
Fringe spacing	$3.75 \mu\text{m}$
Beam spacing	8.44 mm
Number of fringes	21.5
Dimensions of the measur. volume	
Major axis	1.91 mm
Minor axis	$80.6 \mu\text{m}$

tab:lda

The APD does not have a variable gain as the commercially used photomultiplier tubes, but on the other hand are more robust and can also provide the required high frequency response. The scattered light was collected directly to the APD, avoiding the use of a fiber optical cable. The circuit board of the APD was connected to an oscilloscope for verification of the signal quality and initial acquisition tests.

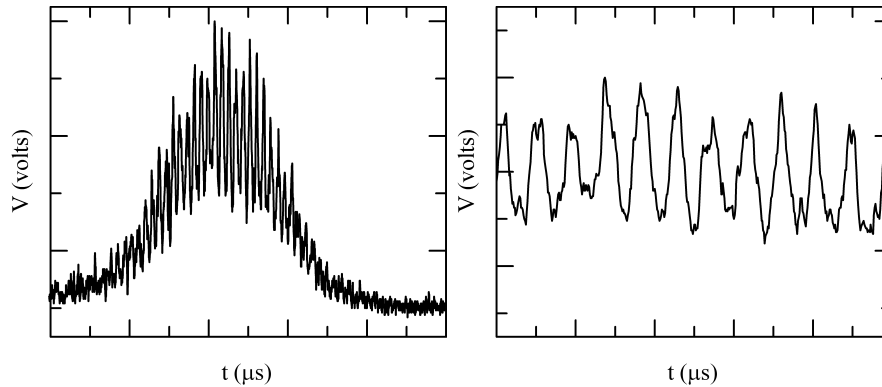


Figure 4. Burst signal measured with the present system: (a) raw signal with pedestal, (b) detail of the Doppler signal showing the periodic zero crossings.

fig:burs

Before attempting to measure an actual flow field, it was crucial to evaluate the system response under fully controlled conditions. For this purpose, the presence of the seeding particles was simulated via a 5 micron tungsten wire fixed to a variable rotating motor. Each revolution of the motor would then generate one burst signal on the APD output signal, as the wire crossed the fringes on the measurement volume. The motor was placed in a traverse with precision of one micron in order to allow accurate positioning of the wire on the measurement volume. Despite the assembling precision was high, the seeding wire could not provide a good repeatability, given its small inertia and the distance required between the motor and the control volume.

The second attempt was to generate the burst signals with the aid of a rotating disk, following the calibration procedure used for the highly accurate metrological LDA systems. This configuration provided very clear, stable and repeatable burst signals. Then, the reference value for validation of the calculated velocity data was given by the measurement of the rotation of the motor and the radial position of the measurement volume.

4. VELOCITY MEASUREMENTS

Typical bursts measured with this system are shown in Fig. 4, where the picture of the right shows the detail of the Doppler signal showing the periodic zero crossings. Once the burst signals have been adequately generated through the optical configuration described in the previous section, a data acquisition and analysis software is required for proper velocity calculations.

In the present work, the APD output has been digitised by a 100 MHz, 16 bit precision, National Instruments A/D board. The LabView platform has been used to write the acquisition and treatment software, as depicted in Fig. 5. The APD signal was then digitally filtered and the Doppler frequency was estimated via a Fast Fourier Transform. The Doppler frequency provided by individual bursts was then multiplied by the distance between the interference fringes, Eq. (1), to provide the calculated disk velocity at the measurement volume.

Reference data obtained with the aid of the rotating disk are now compared with the velocity calculated from the Doppler frequency. Eight different measurement points in the range of 0.6 ms^{-1} to 4.1 ms^{-1} are shown in Table 2 as well as in Fig. 6. The maximum uncertainty observed between the reference velocity and the calculated is around 0.053%. Fig. 6 presents a fit through the origin to the experimental data, showing the very good agreement between reference and measured data.

An attempt has been made to compare these results with measurements provided by the Mini-LDV system from MSE

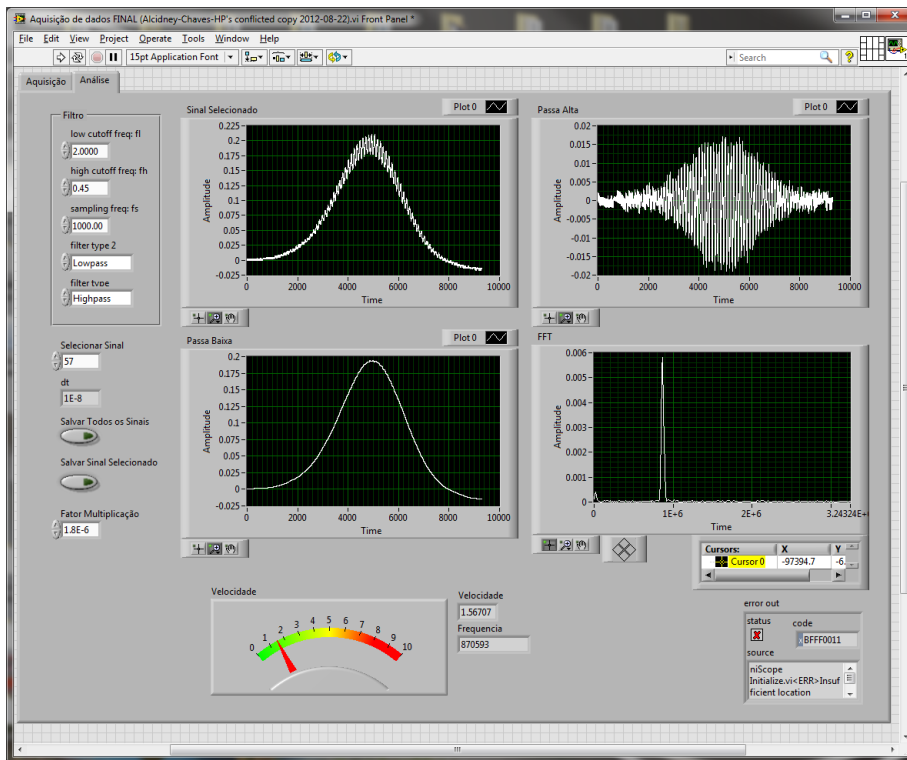


Figure 5. General view of the data acquisition and treatment software interface.

fig:scree

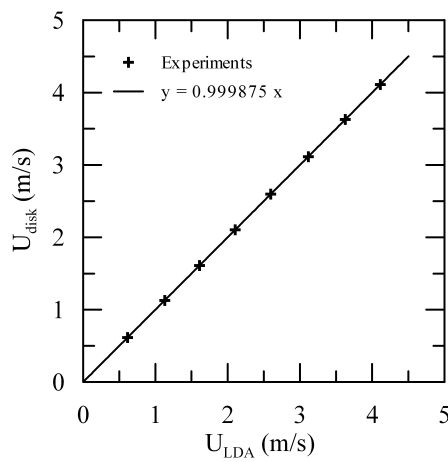


Figure 6. Comparison between the reference velocity provided by the rotating disk and the measured velocity calculated from the Doppler frequency.

fig:comp

Table 2. Comparison between the velocity calculated from the Doppler frequency of measured bursts and the reference velocity from the rotating disk.

Disk Voltage (V)	U_{LDA} (m/s)	U_{disk} (m/s)
2	0.615	0.616
3	1.129	1.126
4	1.610	1.611
5	2.104	2.102
6	2.596	2.597
7	3.116	3.118
8	3.627	3.625
9	4.112	4.112

tab:results

(Modaress, 2000) under the same test conditions. However, for the present optical configuration, the rotating disk scattered too much light, that saturated the Mini-LDV detector and prevented the velocity calculation.

5. FINAL REMARKS

Results presented here show that the working principle of the Laser Doppler Anemometry has been successfully reproduced and velocity measurements on an optical bench could be obtained with a high degree of accuracy. Dedicated software for data acquisition and treatment has been developed and used for mean velocity calculation.

Although the assembly and alignment of the optical configuration from single components is time consuming, the development performed in the present work allows a complete understanding of the laser Doppler anemometry, from the mounting of individual parts to the mean velocity and statistics calculations. The dependence on the use of high cost LDA commercial systems and its black boxes for data processing will consistently decrease as the integrated optical unit is developed.

Furthermore, the optical components can be arranged to fit perfectly the experimental set up dimensions, allowing detailed measurements of wall shear stress (Loureiro et al., 2010) and increased spatial resolution.

The integrated optical unit developed in this work will be test in a horizontal flow loop for the improvement of the data acquisition and analysis software. The results will also be compared with data obtained from commercial LDA systems.

Further developments may provide an improved integrated optical unit that can be used for industrial applications.

6. ACKNOWLEDGEMENTS

Authors are indebted to Dr. Kim D. Jensen for his invaluable comments and cheerful discussion on the subject. In the course of the research, JBRL benefited from a CNPq Research Fellowship (Grant No 301172/2010-2) and from further financial support through Grant 477354/2011-4. The work was initially supported by CNPq through Grant No 475759/2009-5.

7. REFERENCES

- Albrecht, H. E., Borys, M., Damasche, N. and Tropea, C., 2003. Laser-Doppler and Phase-Doppler Measurement Techniques, 738 pp., Springer-Verlag.
- Byrne, G. D., James, S. W. and Tatam, R. P., 2004. A single-headed fibre optic laser Doppler anemometer probe for measurement of flow angles. Meas. Sci. Technol., vol. 15, pp. 1–8.
- Durst, F., Melling, A. and Whitelaw, J. H., 1976. Principles and Practice of Laser-Doppler Anemometry. 405 pp.
- Durst, F. and Whitelaw, J. H., 1971. Integrated optical units for laser anemometry. J. Phys. E: Sci. Instrum., pp. 804–808.

Knuhtsen, J., Olldag, E. and Buchhave, P., 1982. Fibre-optic laser Doppler anemometer with Bragg frequency shift utilising polarisation-preserving single-mode fibre. *J. Phys. E: Sci. Instrum.*, Vol. 15, pp. 1188–1191.

Liu, H. T., Kollé, J. J. and Bondurant, P. D., 1922. Development of field-worthy diode laser Doppler velocimeters. *J. Phys. E: Sci. Instrum.*, pp. 1630–1635.

Loureiro, J. B. R., Sousa, F. B. C. C., Zotin, J. L. Z. and Silva Freire, A. P., 2010. The distribution of wall shear stress downstream of a change in roughness, *International Journal of Heat and Fluid Flow*, vol. 31, pp. 785–793.

Modarress, D., 2000. Design and development of miniature and micro-Doppler sensors. *Proceedings of ASME 2000 Fluids Engineering Division, Summer Meeting*.

Tropea, C., 1995. Laser-Doppler anemometry - recent developments and future challenges. *Meas. Sci. Technol.*, pp. 6605-6619.

Yeh, Y. and Cummings, H. Z., 1964. Localized fluid flow measurements with an He-Ne laser spectrometer. *Applied Phys. Letters*, vol. 4, pp. 176–178.